

# Inner horizon instability and the unstable cores of regular black holes

Raúl Carballo-Rubio,<sup>1</sup> Francesco Di Filippo,<sup>2,3</sup> Stefano Liberati,<sup>3,4,5</sup> Costantino Pacilio,<sup>6</sup> and Matt Visser<sup>7</sup>

<sup>1</sup> *Florida Space Institute, University of Central Florida,  
12354 Research Parkway, Partnership 1, Orlando, FL, USA*

<sup>2</sup> *Center for Gravitational Physics,  
Yukawa Institute for Theoretical Physics,  
Kyoto University, Kyoto 606-8502, Japan*

<sup>3</sup> *SISSA - International School for Advanced Studies,  
Via Bonomea 265, 34136 Trieste, Italy*

<sup>4</sup> *IFPU - Institute for Fundamental Physics of  
the Universe, Via Beirut 2, 34014 Trieste, Italy*

<sup>5</sup> *INFN Sezione di Trieste, Via Valerio 2, 34127 Trieste, Italy*

<sup>6</sup> *Dipartimento di Fisica, “Sapienza” Università di Roma & Sezione INFN Roma1,  
Piazzale Aldo Moro 5, 00185, Roma, Italy*

<sup>7</sup> *School of Mathematics and Statistics, Victoria University of Wellington,  
PO Box 600, Wellington 6140, New Zealand*

## Abstract

We discuss the generalization of the Ori model to black holes with generic inner horizons (with arbitrary location and surface gravity), analyzing the behavior of the metric around these inner horizons under the influence of both a decaying ingoing flux of energy satisfying Price’s law and an outgoing flux described by a null shell. We show that the exact solution for the late-time evolution obtained by Ori is valid for all spacetimes in which the Misner–Sharp mass is assumed to be linearly proportional to the time-dependent metric perturbations introduced. We then consider generic situations in which this linear proportionality is not assumed, obtaining asymptotic analytical expressions and performing numerical integrations that show how the exponential divergence associated with mass inflation is generically replaced at late times by a power-law divergence. We emphasize that all these geometries initially experience a first phase in which mass inflation proceeds exponentially, and describe the physical implications that follow for generic regular black holes. The formalism used also allows us to make some remarks regarding the early-time transients associated with a positive cosmological constant, known to modify the late-time behavior of ingoing perturbations from Price’s law to an exponential decay. Finally we compare our analysis with that in arXiv:2010.04226v1, and illustrate specific shortcomings in the latter work that explain the differing results and, in particular, make it impossible for that analysis to recover the well-known Ori solution for Reissner–Nordström backgrounds.

## I. INTRODUCTION

Singularity theorems [1–3] demonstrate that, within the framework of standard general relativity, singular black holes are unavoidably formed as the end state of gravitational collapse. Observational tests of black hole spacetimes coming from the detection of gravitational waves emitted by the merger of two black holes [4–8] are so far in perfect agreement with the predictions of general relativity. However, there is still room for alternatives to classical black holes [9, 10], a consideration that becomes more pertinent given that it is reasonable to assume that singularities will be tamed once quantum gravity effects are taken into consideration, which naturally leads to some of these alternatives [11, 12].

Among the different classes of black hole mimickers, a very simple approach consists of replacing the singularity with a regular core without necessarily introducing substantial long-range modifications to the geometry. The price to pay for such a conservative approach is the introduction of an inner horizon [11, 12] whose stability is not guaranteed. In fact, it is well known that inner horizons in general relativity are generically unstable under small perturbations (see *e.g.* [13–15]). Such instability has indeed been found in the context of regular black holes, first for a particular model [16] and then for a generic regular black hole metric [17]. While these analyses capture the main physical ingredients, they consider a somewhat idealized scenario consisting of two non-interacting null shells on top of a static background.

Recent work [18], which aimed to extend the result of Ori’s work for Reissner–Nordström black holes [14] to regular black hole spacetimes, claims that a less idealized configuration of perturbations would lead to a stable inner horizon. However, we point out a technical issue in the analysis of [18], and that the inner horizon of a regular black hole is indeed generically unstable. To this end, in sec. II we extend Ori’s calculation to a generic spherically symmetric metric. In sec. III we repeat the analysis using the formalism of [18], as this formalism may provide a more straightforward physical interpretation and it is better suited to numerically solve the exact time evolution of the geometry. In sec. IV we consider the role of the cosmological constant, showing that also in this case the instability is present, and that it could become sub-exponential at most at late times (when the backreaction would be already non-negligible anyway). Finally, in sec. V we solve numerically the differential equations governing the growth of instability for many specific choices of spacetimes, and we show that the solutions are in agreement with the analytical treatment of the previous sections. Our conclusions are summarized in sec. VI.

## II. GENERALIZED ORI MODEL

In reference [14] Ori developed a model to describe the dynamical evolution of the neighborhood of the inner horizon of a Reissner–Nordström black hole under perturbations, in order to explicitly analyze the singularity generated by the mass-inflation instability. The Ori model can be easily generalized to any (singular or non-singular) spacetime with a metric of the form

$$ds^2 = -f(v, r)dv^2 + 2dvdr + r^2d\Omega^2. \quad (1)$$

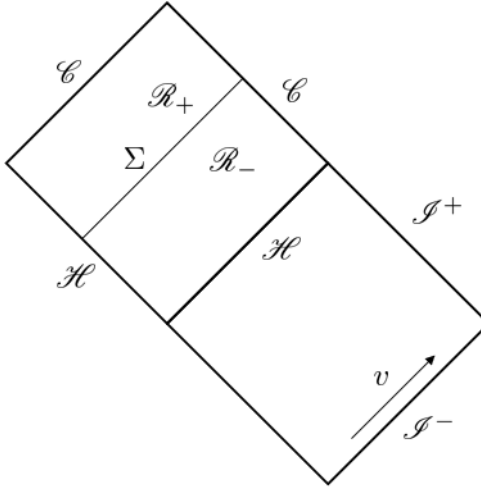


Figure 1: Relevant sections of the Penrose diagram of a regular black hole. The shell  $\Sigma$  divides the spacetime in two regions  $\mathcal{R}_-$  and  $\mathcal{R}_+$ .  $\mathcal{H}$  denotes the event horizon while  $\mathcal{C}$  denotes the Cauchy horizon.

Most of the derivation can be worked out only using the parameterization  $f(v, r) = 1 - 2M(v, r)/r$  in terms of the Misner–Sharp mass  $M(v, r)$ . At this point in the discussion we do not need to assume any specific form of the Misner–Sharp mass, but only that its radial dependence is such that the geometry contains an inner horizon or, equivalently, that  $f(v, r)$  has an even number of zeroes, and that all its dependence on  $v$  enters through a single-variable function  $m(v)$  which coincides with the value of the Misner–Sharp mass at large values of  $r$ , namely

$$M(v, r) = M(m(v), r), \quad (2)$$

with

$$m(v) = \lim_{r \rightarrow +\infty} M(v, r). \quad (3)$$

Well-known examples include the Vaidya–Reissner–Nordström spacetime in which  $M(m, r) = m - e^2/2r$ , or the Hayward spacetime in which  $M(m, r) = mr^3/(r^3 + 2m\ell^2)$  [19].

Following reference [14], we now consider a dynamical model of a null shell  $\Sigma$  which divides the black hole into two subregions  $\mathcal{R}_-$  and  $\mathcal{R}_+$ , such that  $\mathcal{R}_-$  is on the same side of  $\mathcal{I}^-$ , as shown by the Penrose diagram in fig. 1. Therefore we can parametrize  $\mathcal{R}_-$  by the same advanced null coordinate  $v_-$  of  $\mathcal{I}^-$ , while we shall choose a distinct null coordinate  $v_+$  to parametrize  $\mathcal{R}_+$ . By continuity, the radial coordinate  $r$  is the same on both regions, while the mass function  $m(v)$  depends on the region, so that we shall distinguish  $m_-(v_-)$  and  $m_+(v_+)$ . On the other hand, the matching conditions imply that both  $v_-$  and  $v_+$  can be expressed *on*  $\Sigma$  in terms of a single affine coordinate  $\lambda$  [20]. We will define  $\lambda$  in such a way that it is negative and  $\lambda \rightarrow 0$  when  $v_- \rightarrow \infty$ . Additionally, the radius of the shell can be expressed as a function  $R(\lambda)$  of the affine parameter.

The functional form of  $m_-(v_-)$  is dictated by Price's law [21, 22] to be

$$m_-(v_-) = m_0 + \delta m = m_0 - \frac{\beta}{v_-^p}. \quad (4)$$

When  $v_- \rightarrow \infty$ , the shell crosses the corresponding inner horizon  $r_0$ , which is implicitly defined by

$$\lim_{\lambda \rightarrow 0} R = r_0; \quad (5a)$$

$$\lim_{\lambda \rightarrow 0} f_-(\lambda, R) = 0; \quad (5b)$$

where  $R \equiv R(\lambda)$  is the radius of the shell and  $f_-(\lambda, R) = f(M(m_-(\lambda), R), R)$ . It is convenient to define the surface gravity in  $\mathcal{R}_-$  at  $\lambda = 0$  as

$$\kappa_0 = \frac{1}{2} \lim_{\lambda \rightarrow 0} \left. \frac{\partial f_-(\lambda, r)}{\partial r} \right|_{r=R(\lambda)}. \quad (6)$$

We now set up the basic ingredients for the discussion of the generalized Ori model. It can be shown that the matching conditions on  $\Sigma$  in eqs. (7)–(9) of [14] generalize, respectively, to

$$z_i R' = \frac{R}{2} f_i(v_i, R); \quad (7a)$$

$$v_i(\lambda) = \int^\lambda d\lambda \frac{R}{z_i}; \quad (7b)$$

$$z_i(\lambda) = Z_i + \frac{1}{2} \int^\lambda d\lambda \left( f_i(\lambda, R) + R \frac{\partial f_i}{\partial r}(\lambda, R) \right); \quad (7c)$$

where  $z_i = R/v_i'$ , the index  $i$  takes two values  $+$  and  $-$  (for the two regions  $\mathcal{R}_+$  and  $\mathcal{R}_-$ , respectively), and a prime denotes differentiation with respect to  $\lambda$ . The quantity  $Z_i$  is an integration constant, while we omitted a similar integration constant in (7b) because it is irrelevant. These equations are valid on both sides of the ingoing null shell. Now, in region  $\mathcal{R}_-$ , we can expand eq. (7c) around  $\lambda = 0$  to obtain

$$z_-(\lambda) = Z_- - r_0 |\kappa_0| \lambda + \mathcal{O}(\lambda^2). \quad (8)$$

However, given that  $\lim_{\lambda \rightarrow 0} v_- = \infty$ , it follows from eq. (7b) that  $Z_- = 0$ , otherwise  $v_-$  would tend to a constant proportional to  $1/Z_-$ , and therefore (hereafter, for simplicity, we will use  $v$  in place of  $v_-$ )

$$v(\lambda) = -\frac{1}{|\kappa_0|} \ln |\lambda| + \mathcal{O}(\lambda^0). \quad (9)$$

Notice that the derivation of (8) and (9) proceeded exactly as in reference [14]. Furthermore, eq. (7a) in region  $\mathcal{R}_-$  can be written as a differential equation in  $v$  as

$$\frac{dR(v)}{dv} = \frac{1}{2} f_-(m_-(v), R(v)). \quad (10)$$

We can perform a Taylor expansion of  $f_-$  around the values  $m_- = m_0$  and  $R = r_0$  at  $v = \infty$  to obtain

$$\frac{d\delta R(v)}{dv} = -\frac{A}{r_0}\delta m(v) - |\kappa_0|\delta R(v) + \mathcal{O}(\delta m^2, \delta m\delta R, \delta R^2), \quad (11)$$

where we have written  $R(v) = r_0 + \delta R(v)$  and  $A = \partial M_-/\partial m_-|_{m_- = m_0, r = r_0}$ . The general solution to the differential equation above (neglecting subleading orders) is given by

$$\delta R(v) = c_1 e^{-|\kappa_0|v} - \frac{A}{r_0} e^{-|\kappa_0|v} \int d\tilde{v} \delta m(\tilde{v}) e^{|\kappa_0|\tilde{v}}, \quad (12)$$

where  $c_1$  is an integration constant. This equation is valid for a generic  $\delta m(v)$ . If we further consider the functional form of  $\delta m(v)$  from eq. (4) we obtain

$$\begin{aligned} \delta R(v) &= c_1 e^{-|\kappa_0|v} + \frac{A\beta}{|\kappa_0|r_0 v^p} \sum_{k=0}^{\infty} \left[ \frac{(p+k-1)!}{(p-1)!} \frac{1}{|\kappa_0|^k v^k} \right] \\ &= \frac{A\beta}{|\kappa_0|r_0 v^p} \left\{ 1 + \frac{p}{|\kappa_0|v} + \frac{p(p+1)}{|\kappa_0|^2 v^2} + \mathcal{O}(v^{-3}) \right\}. \end{aligned} \quad (13)$$

Let us now consider the evolution of the metric functions in region  $\mathcal{R}_+$  on its boundary  $\Sigma$ , hence as functions of  $\lambda$  only (alternatively,  $v$ ). One can manipulate eqs. (7a) and (7c) for  $i = +$  to obtain

$$\frac{df_+(\lambda, R)}{d\lambda} = R' \frac{\partial f_+(\lambda, r)}{\partial r} \Big|_{r=R} + \frac{R''}{R'} f_+(\lambda, R), \quad (14)$$

or equivalently, as a differential equation in  $v$ ,

$$\begin{aligned} \frac{dM_+(v, R)}{dv} &= R_{,v} \frac{\partial M_+(v, r)}{\partial r} \Big|_{r=R} - \left( \frac{\lambda_{,vv}}{\lambda_{,v}} - \frac{R_{,vv}}{R_{,v}} \right) \left( M_+(v, R) - \frac{R}{2} \right) \\ &= R_{,v} \frac{\partial M_+(v, r)}{\partial r} \Big|_{r=R} + \left( |\kappa_0| - \frac{p+1}{v} + \mathcal{O}(v^{-2}) \right) \left( M_+(v, R) - \frac{R}{2} \right). \end{aligned} \quad (15)$$

In the equation above the  $v$  subindices denote differentiation with respect to this variable. In the case of Reissner–Nordström,

$$\frac{\partial M_+(v, r)}{\partial r} \Big|_{r=R} = \frac{e^2}{2R^2}, \quad (16)$$

so the first term of the right-hand side of eq. (15) does not depend on  $M_+$  and the equation displays (exponentially) inflating solutions with leading behaviour

$$M_+(v, R(v)) \propto \frac{e^{|\kappa_0|v}}{v^{p+1}}. \quad (17)$$

This is precisely the exact solution obtained by Ori [14]. More generally, we see that this result by Ori is recovered unchanged for a wider family of geometries satisfying the linear ansatz  $M(v, r) = g_1(r)m(v) + g_2(r)$ , which includes for instance the Bardeen metric for a regular black hole.

Not all metrics potentially of interest are covered by this linear ansatz. For instance, in the case of the regular black hole described by the Hayward metric [19], the functional form of  $M(m, r) = mr^3/(r^3 + 2m\ell^2)$  implies that

$$\frac{\partial M}{\partial r} = \frac{6\ell^2}{r^4} M^2. \quad (18)$$

While these more general situations can be analyzed using the equations above, it is not difficult to see, either using eq. (15) or eq. (7) directly, that the linear ansatz for  $M(v, r)$  is necessary in order to derive Ori's solution in eq. (17). We will discuss these more general situations in more detail, using both analytical and numerical methods, after an equivalent formalism is described in the next section.

### III. ALTERNATIVE DERIVATION

It is instructive to derive the same results with a slightly different, although equivalent, formalism. Moreover, this will allow us to critically analyze the results presented in reference [18]. The analysis of this section will closely follow the discussion in that work up to the point where we correct a technical error therein. We will then discuss how this technical error invalidates the conclusions presented in reference [18].

The setting is the same as in the Ori model discussed in the previous section, and we will therefore use the same notation. The main difference in this section is the way in which the gluing of the two spacetime regions along  $\Sigma$  is dealt with. Instead of using the existence of a common (for both regions) affine parameter  $\lambda$ , we will focus on the junction conditions at the shell [20]

$$[T_\mu{}^\nu s^\mu s_\nu] = 0, \quad (19)$$

where  $T_\mu{}^\nu$  is the effective stress energy tensor obtained by imposing Einstein's equations on both regions of the spacetime, and

$$s^\mu = (2/f_\pm, 1, 0, 0) \quad (20)$$

is the outgoing null normal to the shell. The relevant components of the stress energy tensor are

$$T_v{}^v = -4\pi r^2 \frac{\partial M}{\partial r}, \quad T_v{}^r = 4\pi r^2 \frac{\partial M}{\partial v}, \quad T_r{}^r = -4\pi r^2 \frac{\partial M}{\partial v}. \quad (21)$$

Eq. (19) then becomes

$$\frac{1}{f_+^2} \frac{\partial M_+(v_+, r)}{\partial v_+} \Big|_{r=R(v_+)} = \frac{1}{f_-^2} \frac{\partial M_-(v_-, r)}{\partial v_-} \Big|_{r=R(v_-)}. \quad (22)$$

We can eliminate the  $v_+$  dependence from this equation noting that along a null trajectory

$$dr = \frac{1}{2} f_\pm dv_\pm, \quad (23)$$

or, equivalently,

$$\frac{dv_+}{dv_-} = \frac{f_-}{f_+}. \quad (24)$$

Using this equation in order to relate the total derivatives of  $M_+$  with respect to  $v_+$  and  $v_-$  allows us to write eq. (22) as

$$\frac{1}{f_+} \frac{\partial M_+}{\partial v} \Big|_{r=R(v)} = \frac{1}{f_-} \frac{\partial M_-}{\partial v} \Big|_{r=R(v)} \quad (25)$$

where, as in the previous section, we use  $v$  in place of  $v_-$ . We emphasize that, when evaluating eq. (25) on the shell  $\Sigma$ , the partial derivatives with respect to  $v$  must be taken before imposing  $r = R(v)$  on  $\Sigma$  (one would be calculating total derivatives otherwise, thus changing the content of the equation). Crucially, this observation lies at the core of the technical flaw in [18], as it will be discussed in more detail at the end of this section: indeed, in deriving their eq. (13), the authors imposed the condition  $r = R(v)$  inside the partial derivative signs in eq. (25).

Given that we are following the evolution of  $M(v, r)$  on the trajectory  $r = R(v)$  or, in other words, we are solving a coupled system of differential equations for  $R(v)$  and  $M(v, R(v))$ , we cannot directly integrate eq. (25) because it involves partial derivatives with respect to  $v$ . Instead we need to consider an equivalent equation involving total derivatives. To this end, let us note that

$$\frac{dM_+(v, R(v))}{dv} = \frac{\partial M_+(v, r)}{\partial v} \Big|_{r=R(v)} + \frac{\partial M_+(v, r)}{\partial r} \Big|_{r=R(v)} \frac{dR(v)}{dv}. \quad (26)$$

Using eq. (25), the above equation can be rewritten as

$$\frac{dM_+(v, R(v))}{dv} = \frac{f_+}{f_-} \frac{\partial M_-(v, r)}{\partial v} \Big|_{r=R(v)} + R_{,v} \frac{\partial M_+(v, r)}{\partial r} \Big|_{r=R(v)}. \quad (27)$$

Consider now the identity

$$\frac{1}{f_-} \frac{\partial M_-(v, r)}{\partial v} \Big|_{r=R(v)} = \frac{1}{2R_{,v}} \frac{\partial M_-(v, r)}{\partial m_-} \Big|_{r=R(v)} \frac{dm_-(v)}{dv} \quad (28)$$

which holds true on  $\Sigma$  due to the functional form of the Misner–Sharp mass,  $M(v, r) = M(m(v), r)$ , and the equation of motion for the null shell  $\Sigma$ , namely eq. (10). Moreover, in eq. (13) we obtained the solution of the equation of motion for the null shell, which using the derivative of eq. (4) can be written as

$$R_{,v} = -\frac{A}{|\kappa_0|^2 r_0} \frac{dm_-(v)}{dv} \left( |\kappa_0| + \frac{p+1}{v} \right) + \mathcal{O}(v^{-p-3}). \quad (29)$$

It is then straightforward to see that the derivatives of the function  $m_-(v)$  cancel on the right-hand side of eq. (28), while the definition  $A = \partial M_- / \partial m_-|_{m_- = m_0, r = r_0}$  allow us to further simplify the resulting expression to

$$\begin{aligned} \frac{1}{f_-} \frac{\partial M_-(v, r)}{\partial v} \Big|_{r=R(v)} &= -\frac{r_0 |\kappa_0|^2}{2} \left( |\kappa_0| + \frac{p+1}{v} \right)^{-1} + \mathcal{O}(v^{-2}) \\ &= -\frac{r_0}{2} \left( |\kappa_0| - \frac{p+1}{v} \right) + \mathcal{O}(v^{-2}). \end{aligned} \quad (30)$$

As a consequence we obtain

$$\frac{dM_+(v, R(v))}{dv} = \left( |\kappa_0| - \frac{p+1}{v} + \mathcal{O}(v^{-2}) \right) \left\{ M_+(v, R(v)) - \frac{r_0}{2} \right\} + R_{,v} \frac{\partial M_+}{\partial r} \Big|_{r=R(v)}. \quad (31)$$

If  $\partial M_+/\partial r$  is proportional to  $M_+$ , namely  $M_+(v, r) = g_1(r)m_+(v) + g_2(r)$ , the last term becomes subdominant at late times due to being multiplied by  $R_{,v} = \mathcal{O}(v^{-p-1})$  terms and we have

$$M_+(v, R(v)) = c_2 \frac{e^{|\kappa_0|v}}{v^{p+1}} [1 + \mathcal{O}(v^{-1})] + \mathcal{O}(v^0), \quad (32)$$

where  $c_2$  is an integration constant. Hence, we reproduce Ori's result. However, if  $\partial M_+/\partial r$  is not linear in  $M_+$ , the differential equation (31) becomes nonlinear and the last term on its right-hand side may drive the evolution at late times, thus modifying the exponential behavior associated with mass inflation. Hence, the analysis must proceed in a case-by-case basis for these more general situations.

For instance let us consider the case where  $\partial M_+/\partial r$  is polynomial in  $M_+$ . We would get

$$\frac{dM_+(v, R(v))}{dv} = \left( |\kappa_0| - \frac{p+1}{v} + \mathcal{O}(v^{-2}) \right) \left\{ M_+(v, R(v)) - \frac{r_0}{2} \right\} - \frac{\gamma}{v^{p+1}} M_+^n(v, R(v)). \quad (33)$$

for some given constants  $\gamma$  and  $n$  depending on the specific metric under consideration. The behavior of the solution of this differential equation depends on the sign of  $\gamma$ . It is possible to show, for  $\gamma < 0$ , that  $M_+(v, R(v))$  diverges for a finite value of  $v$ . On the other hand, for  $\gamma > 0$  we can solve this differential equation in different regimes. At early times the first term on the right hand side dominates the dynamics, and this equation predicts an exponential growth of  $M_+(v, R(v))$ , up to a critical time  $v_0$  for which

$$M_+^{n-1}(v_0, R(v_0)) \approx \frac{|\kappa_0|}{\gamma} v_0^{p+1}. \quad (34)$$

From that point on the first and the second term of the right hand side assume comparable values and the growth is polynomial rather than exponential,

$$M_+^{n-1}(v, R(v)) \propto v^{p+1}, \quad v \gg v_0. \quad (35)$$

As a concrete example, let us consider Hayward's metric for which the relation (18) allows us to write

$$\frac{dM_+(v, R(v))}{dv} \simeq |\kappa_0| M_+(v, R(v)) - \gamma \frac{M_+^2(v, R(v))}{v^{p+1}} - \frac{r_0 |\kappa_0|}{2}, \quad (36)$$

where the symbol  $\simeq$  means that we are neglecting subdominant terms in the  $v \rightarrow \infty$  limit, and

$$\gamma = \frac{6p\beta\ell^2}{|\kappa_0|} \frac{r_0}{(2m_0\ell^2 + r_0^3)^2}. \quad (37)$$

By neglecting the last term on the right hand side, the solution of (36) is given by

$$M_+(v, R(v)) \approx \frac{e^{|\kappa_0|v} v^p}{c_1 v^p - (-v)^p |\kappa|^{p-1} \gamma \Gamma(-p, -|\kappa_0|v)}. \quad (38)$$

Expanding the incomplete Gamma function at late times we obtain

$$M_+(v, R(v)) \approx \frac{|\kappa_0|}{\gamma} v^{p+1}, \quad (39)$$

in perfect agreement with eq. (35). Therefore, the growth rate of the instability is slowed down, becoming polynomial rather than exponential at late times. However, it is reasonable to expect that this polynomial behaviour will not have any physical consequence, as it occurs beyond the validity of our linear analysis and after a certain timescale during which the Misner–Sharp mass has already become substantially large in an exponential fashion. Indeed, assuming that the regularization scale  $\ell$  satisfies the condition  $\ell \ll m_0$ , (as would be the case if, for instance,  $\ell$  is given by the Planck length), and substituting (37) into (34) we see that  $M_+$  grows exponentially up to the critical value

$$M_+(v, R(v)) \approx \frac{|\kappa_0|^2 (2m_0 \ell^2 + r_0^3)^2}{r_0 \ell^2} \frac{v_0^{p+1}}{6p\beta} \sim \frac{m_0^2}{\ell} \frac{v_0^{p+1}}{6p\beta}, \quad (40)$$

where we have used

$$r_0 \sim |\kappa_0|^{-1} \sim \ell. \quad (41)$$

Eq. (40) implies

$$\frac{M_+(v, R(v))}{m_0} \sim \frac{m_0}{\ell} \frac{v_0^{p+1}}{6p\beta} \gg 1. \quad (42)$$

So the transition between exponential and polynomial regimes happens when the backreaction of the perturbation on the background geometry is already very large due to an initial phase of exponential growth of the Misner–Sharp mass, and at this stage we expect nonlinear effects to become relevant and supersede our linear treatment. It is also important to keep in mind that, in any case,  $M_+(v, R(v))$  is always divergent.

Let us now pause for a brief moment to understand why reference [18] fails to capture the divergent nature of  $M_+(v, R(v))$  that we have described above. As previously mentioned, in deriving eq. (13) of reference [18], the condition  $r = R(v)$  was imposed inside the derivatives of eq. (25). That is, the partial derivative is effectively replaced with a total derivative. Therefore, eq. (27) is (incorrectly) modified into

$$\begin{aligned} \frac{dM_+(v, R(v))}{dv} &= \frac{f_+}{f_-} \left( \frac{\partial M_-(v, r)}{\partial v} \bigg|_{r=R(v)} + \frac{\partial M_-(v, r)}{\partial r} \bigg|_{r=R(v)} \frac{dR(v)}{dv} \right) \\ &= \frac{f_+}{f_-} \left( \frac{\partial M_-(v, r)}{\partial v} \bigg|_{r=R(v)} + \frac{f_-}{2} \frac{\partial M_-(v, r)}{\partial r} \bigg|_{r=R(v)} \right). \end{aligned} \quad (43)$$

In order to extract the leading behavior encapsulated in this equation let us note that the definition of the surface gravity of the inner horizon,

$$\frac{\partial [M_-(v, r)/r]}{\partial r} \bigg|_{r=R(v)} = |\kappa_0| + \mathcal{O}(v^{-p}), \quad (44)$$

implies that

$$\frac{\partial M_-(v, r)}{\partial r} \Big|_{r=R(v)} = \frac{M_-(v, R(v))}{r_0} + r_0 |\kappa_0| + \mathcal{O}(v^{-p}). \quad (45)$$

Using the relation above, together with eqs. (28) and (29), we can therefore write

$$\begin{aligned} & \frac{\partial M_-(v, r)}{\partial v} \Big|_{r=R(v)} + \frac{f_-}{2} \frac{\partial M_-(v, r)}{\partial r} \Big|_{r=R(v)} \\ &= \frac{\partial M_-(v, r)}{\partial v} \Big|_{r=R(v)} - \frac{1}{r_0 |\kappa_0|} \frac{\partial M_-(v, r)}{\partial v} \Big|_{r=R(v)} \left\{ \frac{M_-(v, R(v))}{r_0} + r_0 |\kappa_0| + \mathcal{O}(v^{-p}) \right\} \\ &= -\frac{1}{r_0^2 |\kappa_0|} \frac{\partial M_-(v, r)}{\partial v} \Big|_{r=R(v)} \left\{ M_-(v, R(v)) + \mathcal{O}(v^{-p}) \right\}. \end{aligned} \quad (46)$$

This implies that the leading behavior of the incorrect expression (43) is encapsulated in the equation

$$\frac{dM_+(v, R(v))}{dv} \simeq \frac{M_-(v, R(v))}{2r_0} f_+ = \frac{M_-(v, R(v))}{2r_0} - \frac{M_-(v, R(v))}{r_0^2} M_+(v, R(v)). \quad (47)$$

This differential equation does not have growing exponential solutions, but, due to the sign of the second term, decaying ones. In fact, its general solution at leading order is

$$M_+(v, R(v)) \simeq \frac{r_0}{2} + c_1 e^{-M_0 v / r_0^2}, \quad (48)$$

where we have defined the constant  $M_0 = M_-(m_0, r_0)$ . In particular,  $M_+(v, R(v))$  tends to the finite value  $r_0/2$  for  $v \gg r_0^2/M_0$ . Finally, let us note, as a further evidence of something wrong with eq. (43), that, exactly for the aforementioned reasons (and also due to the fact that for the discussion above to work it is not necessary to select an ansatz for the Misner–Sharp mass  $M(m, r)$ ), it also fails to reproduce the well known instability of the inner horizon of a standard Reissner–Nordström black hole.

#### IV. ROLE OF THE COSMOLOGICAL CONSTANT

In the discussion so far we have ignored the role of the cosmological constant. There is a very simple and intuitive reason behind this decision. The instability we have discussed originates close to the inner horizon, where the energy density is Planckian and the role of the cosmological constant is completely negligible. However, in the presence of a non-zero cosmological constant, the late time behavior of the perturbation is no longer described by Price’s law (4), but has an exponential decay [23, 24] characterized by

$$m_-(v) = m_0 + \delta m(v) = m_0 - \alpha e^{-\omega_I v}, \quad (49)$$

where  $\omega_I > 0$  is the imaginary part of the least damped quasinormal mode. This modification only affects the extremely late time behavior of the perturbation, and the very small value of the cosmological constant of our universe implies that the fall-off of the perturbations

follows the polynomial Price's law of eq. (4) for a very long time. Therefore in our universe the instability described in the previous sections will arise well before the cosmological constant could play any significant role. However, it is interesting from the theoretical side to investigate whether or not the values of the cosmological constant and of the black hole parameters can be fine tuned, in such a way that the inner horizon does not become unstable.

Using eq. (49), eq. (12) allows us to obtain

$$\delta R(v) = c_1 e^{-|\kappa_0|v} + \frac{A\alpha}{r_0(|\kappa_0| - \omega_I)} e^{-\omega_I v} \quad (50)$$

where  $c_1$  is an integration constant. This modifies the rate at which  $f_-$  approaches zero which, let us recall, due to eq. (10) is given by the derivative of the expression right above. Eq. (27) can now be written as

$$\frac{dM_+(v, R(v))}{dv} \simeq \frac{f_+ A \alpha \omega_I e^{-\omega_I v}}{-2|\kappa_0|c_1 e^{-|\kappa_0|v} - 2\omega_I A \alpha e^{-\omega_I v}/r_0(|\kappa_0| - \omega_I)} + \frac{f_-}{2} \frac{\partial M_+(v, r)}{\partial r} \Big|_{r=R(v)}. \quad (51)$$

We have to analyze the cases  $|\kappa_0| > \omega_I$  and  $|\kappa_0| < \omega_I$  independently. For  $|\kappa_0| > \omega_I$  we have

$$\frac{dM_+(v, R(v))}{dv} \simeq \frac{r_0(|\kappa_0| - \omega_I) (2M_+(v, R(v))/r_0 - 1)}{2} + \frac{f_-}{2} \frac{\partial M_+(v, r)}{\partial r} \Big|_{r=R(v)}. \quad (52)$$

If  $\partial_r M_+$  is linear in  $M_+$  the last term can be neglected leading to

$$M_+(v, R(v)) \propto e^{(|\kappa_0| - \omega_I)v}. \quad (53)$$

This result has a simple physical interpretation. We have the same blueshift factor  $e^{|\kappa_0|v}$  that we had in the absence of the cosmological constant, while the polynomial decay is replaced by the exponential decay described in equation (49).

Let us now study the case in which  $\partial_r M_+$  is polynomial in  $M_+$ . We have

$$\frac{dM_+(v, R(v))}{dv} \simeq (|\kappa_0| - \omega_I) M_+(v, R(v)) - \gamma e^{-\omega_I v} M_+^n(v, R(v)) - r_0(|\kappa_0| - \omega_I). \quad (54)$$

The late-time behavior of the solution of this differential equation describes an exponential instability

$$M_+(v, R(v)) \propto e^{\omega_I v/(n-1)}. \quad (55)$$

Finally, for  $|\kappa_0| < \omega_I$  we have

$$\frac{dM_+(v, R(v))}{dv} \simeq \frac{(2M_+(v, R(v))/r_0 - 1)}{2|\kappa_0|} A \alpha e^{-(\omega_I - |\kappa_0|)v} - 2|\kappa_0| e^{-|\kappa_0|v} \frac{\partial M_+(v, r)}{\partial r} \Big|_{r=R(v)}. \quad (56)$$

The exact form of the solution depends on the specific choice of the metric. However, the asymptotic behavior is generically regular (that is, the Misner–Sharp mass does not diverge asymptotically). The only scenario left to consider is the special case  $|\kappa_0| = \omega_I$ . While this scenario requires some fine tuning to be realized, let us study it for the sake of completeness. The general solution in eq. (12) now reads

$$\delta R = c_1 e^{-|\kappa_0|v} + \frac{\alpha}{r_0} e^{-|\kappa_0|v} v, \quad (57)$$

leading to

$$\frac{dM_+(v, R(v))}{dv} \approx \frac{A\alpha}{v} M_+(v, R(v)) - \frac{A\alpha r_0}{2v} + \frac{f_-}{2} \frac{\partial M_+(v, r)}{\partial r} \Big|_{r=R(v)} \quad (58)$$

If  $\partial_r M_+$  is linear in  $M_+$  we get

$$M_+(v, R(v)) \propto v^{\alpha A}. \quad (59)$$

Therefore, in this case  $M_+(v, R(v))$  exhibits a polynomial divergence.

## V. NUMERICAL ANALYSIS

In this section we provide some explicit numerical solutions of the equations discussed above for some particular choices of the function  $f(v, r)$ . We can use two equivalent methods for the numerical integrations below. The first one is solving eqs. (10) and (25) for the variables  $R(v)$  and  $m_+(v)$ . The other method considers instead the variables  $R(v)$  and  $M_+(r, R(v))$ , solving the system of differential equations given by eqs. (10) and (27). The main advantage of the second method is that it uses the Misner–Sharp mass as one of the variables, while the function  $m_+(v)$  used in the first method has no clear physical meaning. We will nevertheless use the first method in order to highlight some of the issues that can arise in specific examples due to this choice of variables.

### Reissner–Nordström black hole

In order to connect our discussion with Ori’s original work, let us start by analyzing the case of a Reissner–Nordström black hole. The metric function reads

$$f_{\pm}(v, r) = 1 - \frac{2m_{\pm}(v)}{r} + \frac{e^2}{r^2}. \quad (60)$$

Then, eq. (25) becomes

$$\frac{m'_+(v)}{R^2 - 2Rm_+(v) + q} = \frac{m'_-(v)}{R^2 - 2Rm_-(v) + q}. \quad (61)$$

The asymptotic time evolution of the mass parameter in the past of the shell is determined by Price’s law (4). Eq. (61) can now be solved numerically. The results of the numerical integration are plotted in fig. 2. As expected, the system develops a mass inflation instability and the Misner–Sharp quasilocal mass diverges exponentially.

### Regular black hole: Hayward

Having reproduced Ori’s results for the case of a Reissner–Nordström black hole, we are now confident in extending the computation for different choices of regular black hole geometries.

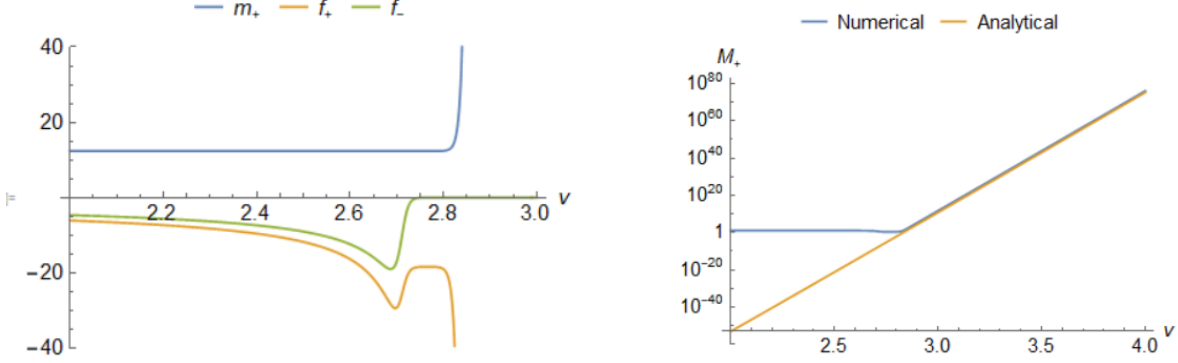


Figure 2: Left: Numerical evolution of the mass parameter  $m_+$  and of the metric functions  $f_\pm$  of a Reissner–Nordström black hole. Right: Comparison between the numerical and the analytical evolution of the Misner–Sharp mass  $M_+$ . In both plots we have used the parameters  $\beta = 1$ ,  $p = 12$ ,  $m_0 = 10$ ,  $q = 5$  with the initial conditions  $R(v = 1) = 5$  and  $m_+(v = 1) = m_0 + 1$ .

The first metric that we are going to analyze is the Hayward regular black hole metric introduced in [19],

$$f_\pm(v, r) = 1 - \frac{2m_\pm(v)r^2}{r^3 + 2m_\pm(v)\ell^2}. \quad (62)$$

The analog of eq. (61) now reads (notice the difference with respect to the incorrect eq. (13) in [18])

$$\frac{m'_+(v)}{(2\ell^2m_+(v) + R^3)(2(\ell^2 - R^2)m_+(v) + R^3)} = \frac{m'_-(v)}{(2\ell^2m_-(v) + R^3)(2(\ell^2 - R^2)m_-(v) + R^3)} \quad (63)$$

We now impose Price’s law (4) for  $m_-(v)$ , and solve numerically for  $m_+(v)$ . The result of the integration is shown in fig. 3. The mass parameter  $m_+(v)$  has a vertical asymptote and, therefore, diverges for finite value of  $v$ . This mathematical divergence does not have any physical implications as the Misner–Sharp mass stays finite. After the asymptote,  $m_+(v)$  changes sign and its late time limit is given by

$$\lim_{v \rightarrow +\infty} m_+(v) = -\frac{r^3}{2\ell^2}. \quad (64)$$

As a consequence, we can see from eq. (62) that the Misner–Sharp mass diverges for large values of  $v$ . However, as shown in the right panel of fig. 3 this divergence is polynomial rather than exponential. As discussed above, an alternative method that can be used to obtain the same results without dealing with the (unphysical) divergence of  $m_+(v)$  at finite  $v$  is changing the variables used for the numerical integration to the physical variables  $R(v)$  and the Misner–Sharp mass  $M_+(r, R(v))$ , and solving the system of differential equations given by eqs. (10) and (27). This leads directly to the right plot in fig. 3.

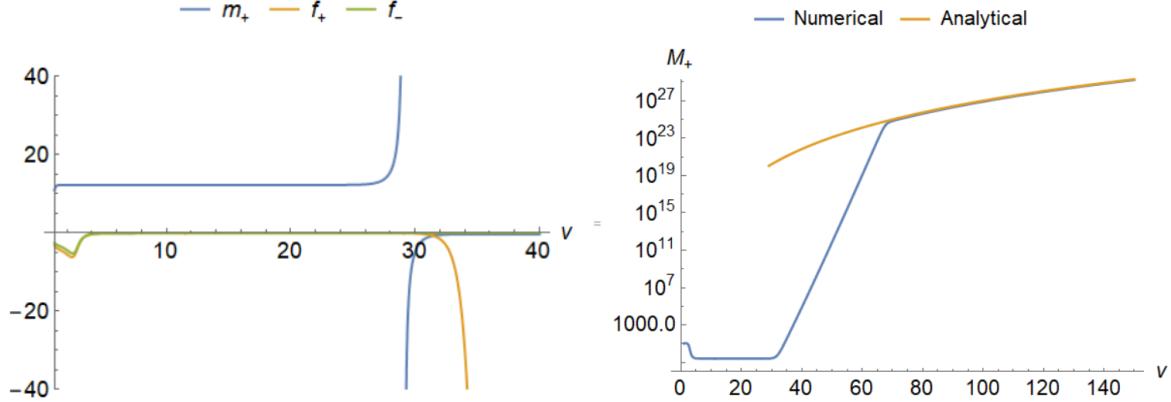


Figure 3: Left: Numerical evolution of the mass parameter  $m_+$  and of the metric functions  $f_\pm$  of a Hayward regular black hole. Right: Numerical evolution of the Misner–Sharp mass. In both plots we picked the parameters  $\beta = 1$ ,  $p = 12$ ,  $m_0 = 10$ ,  $\ell = 0.5$  with the initial conditions  $R(v = 1) = 5$  and  $m_+(v = 1) = m_0 + 1$ .

### Regular black hole: Bardeen

As our next example, let us analyze what happens if we consider the Bardeen metric

$$f_\pm = 1 - \frac{2m_\pm(v)r^2}{(r^2 + \ell^2)^{3/2}}. \quad (65)$$

With this choice we obtain

$$\frac{m'_+(v)}{(\ell^2 + R^2)^{3/2} - 2R^2m_+(v)} = \frac{m'_-(v)}{(\ell^2 + R^2)^{3/2} - 2R^2m_-(v)} \quad (66)$$

As before, we numerically integrate the system of equations for  $m_+$  and  $R$ , and we report the results in fig. 4. Once again, the numerical integration is in perfect agreement with the analytic result: in this case, the mass parameter  $m_+(v)$  diverges exponentially leading to an exponential divergence of the Misner–Sharp mass  $M_+(v, R(v))$ . It is important to remark that the different behaviors of  $m_+(v)$ , a variable that has no direct physical meaning, in the Hayward and Bardeen cases is simply caused by the different functional forms of the Misner–Sharp  $M(m, r)$  as a function of  $m(v)$ . Indeed, in the Hayward case  $m(v)$  appears both in the numerator and denominator of  $M(m, r)$ , while in the Bardeen case  $m(v)$  only appears in the numerator. The Misner–Sharp mass  $M_+(v, R(v))$ , which has a clear physical meaning, displays a divergent behavior in both cases regardless of this difference; in terms of this quantity, the difference between both cases manifests in its different rate of divergence.

### Regular black hole: Dymnikova

Next, let us consider a Dymnikova black hole [25]

$$f_\pm = 1 - \frac{2m_\pm \left(1 - e^{-r^3/\ell^2 m_\pm}\right)}{r}. \quad (67)$$

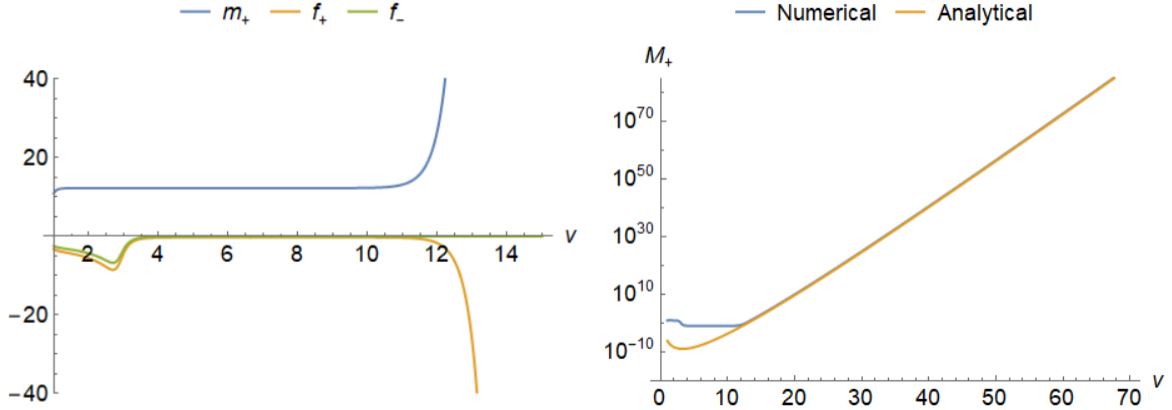


Figure 4: Left: Numerical evolution of the mass parameter  $m_+$  and of the metric functions  $f_\pm$  of a Bardeen regular black hole. Right: Numerical evolution of the Misner–Sharp mass. In both plots we picked the parameters  $\beta = 1$ ,  $p = 12$ ,  $m_0 = 10$ ,  $\ell = 1$  with the initial conditions  $R(v = 1) = 5$  and  $m_+(v = 1) = m_0 + 1$ .

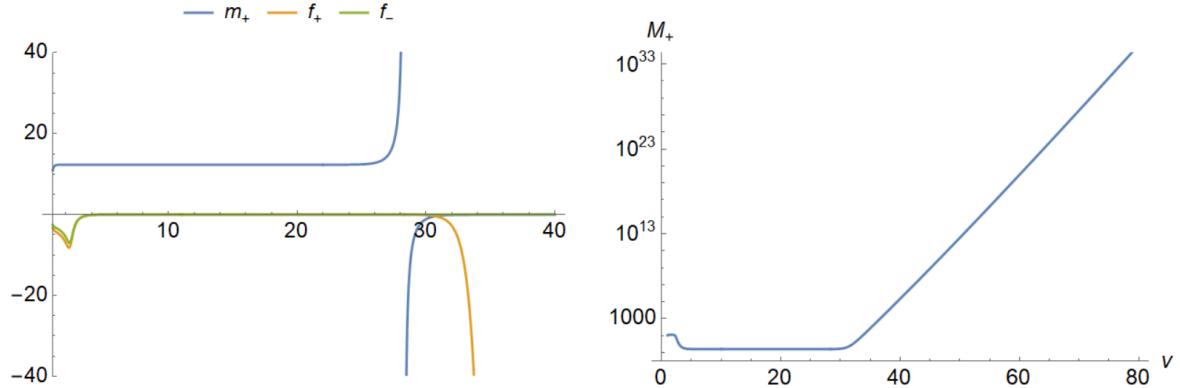


Figure 5: Left: Numerical evolution of the mass parameter  $m_+$  and of the metric functions  $f_\pm$  of a Dymnikova regular black hole. Right: Numerical evolution of the Misner–Sharp mass. In both plots we picked the parameters  $\beta = 1$ ,  $p = 12$ ,  $m_0 = 10$ ,  $\ell = 0.5$  with the initial conditions  $R(v = 1) = 5$  and  $m_+(v = 1) = m_0 + 1$ .

This is a particularly interesting regular black hole metric to consider as the derivative of the Misner–Sharp mass with respect to the radial coordinate is not a polynomial. Therefore, we cannot apply the reasoning of the previous section to analytically determine the late time behavior of  $M_+(r, R(v))$ . As depicted in fig. (5), the numerical integration shows an exponential divergence also for this geometry.

### Regular black hole: Cosmological constant

Finally, let us consider the presence of a non-zero cosmological constant. For this example we consider again the Hayward metric (62) and we assume Price’s law (4) up to a given

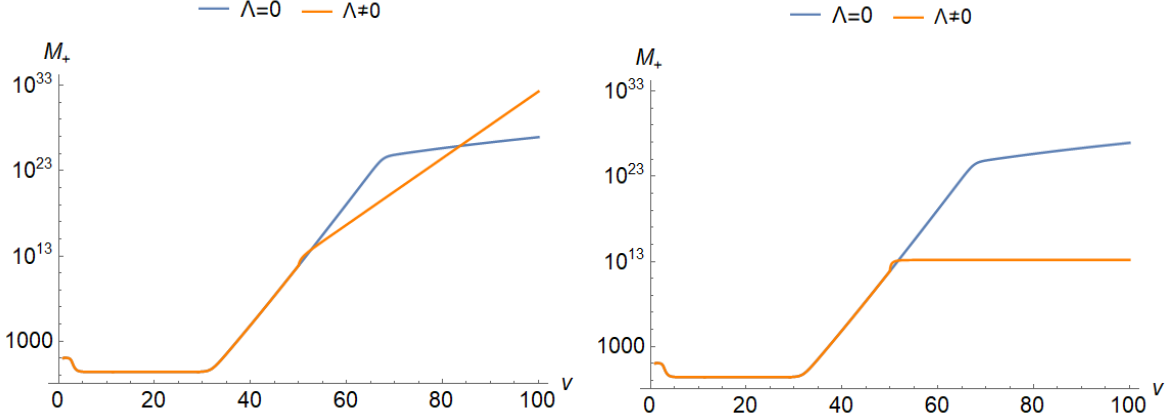


Figure 6: Comparison of the evolution of the Misner–Sharp mass for a Hayward regular black hole, with and without a non-zero cosmological constant. In both plots we picked the parameters  $\beta = 1$ ,  $p = 12$ ,  $m_0 = 10$ ,  $\ell = 0.5$ ,  $R(v = 1) = 5$ , and  $m_+(v = 1) = m_0 + 1$ , leading to a surface gravity  $|\kappa| \approx 1.8$ . Left:  $\omega_I = 1 < |\kappa_0|$ . Right:  $\omega_I = 3 > |\kappa_0|$

time  $v_0$ , and an exponential decay after  $v_0$ . The parameter  $\alpha$  in eq. (49) is picked so that  $m_-$  is continuous, while we have considered two choices of  $\omega_I$ , one for which  $|\kappa_0| > \omega_I$ , and one for which  $|\kappa_0| < \omega_I$ . As shown in fig. 6 the numerical integration agrees with what we expect from the analysis of sec. IV. For  $|\kappa_0| > \omega_I$  the quasilocal mass grows exponentially while, in the case  $|\kappa_0| < \omega_I$  after an exponential phase, the Misner–Sharp mass saturates to a constant value.

## VI. CONCLUSIONS

In this paper, we have analyzed the stability of inner horizons in both singular and regular black holes by extending Ori’s model to a generic spherically symmetric spacetime. We have reproduced Ori’s results and recovered an exponential mass inflation in the case of Reissner–Norström black holes, but we have also extended our analysis to several families of regular black hole geometries, showing that mass inflation at the inner horizon is a robust and very general prediction.

Our findings contradict the conclusions of [18], the discrepancy being due to a technical flaw in the derivation therein. In particular, while in reference [18] the Misner–Sharp mass was found to reach finite values asymptotically in time, we have shown that, once this technical flaw is accounted for, the Misner–Sharp mass becomes divergent for the all the cases analyzed there.

A novel result of our analysis is that the late-time instability can become polynomial instead of exponential. In fact, this happens for well-known regular black hole metrics such as the Hayward metric. However, this regime is always preceded by a period of exponential growth, and we quantified that the onset of the polynomial instability likely occurs when the linear approximation has already broken down. In all the cases that we have considered, there

is always an initial phase in which mass inflation proceeds exponentially, and which persists for large enough times so that the Misner–Sharp mass has already grown considerably. Therefore, the polynomial regime is unlikely to be physically relevant. However, at the moment we cannot completely discard the possibility that it might be possible to cook up a metric for which this transition happens at very early stages, so that the transition to the polynomial regime takes place before the initial exponential growth of the Misner–Sharp becomes significant. The slower polynomial rate of growth would therefore make the inner horizon stable for a longer time.

Similar conclusions apply when a nonvanishing cosmological constant is allowed. While in principle a cosmological constant could stabilize the inner horizon, it requires the imaginary part of the least damped quasinormal mode to be larger than the surface gravity of the inner horizon for every type of perturbation and for every choice of the mass. This is definitely not the case for the Reissner–Norström–de Sitter case [26–29]. Furthermore, even if this condition is realized, the regularization of the instability will only arise after a very long transient in which the curvature invariants grow exponentially. Hence, even if in these hypothetical scenarios the Misner–Sharp mass would be finite, it would reach substantially large values that make imprescindible to consider the backreaction due to the initial exponential phase of mass inflation.

Finally, let us stress that the instability of the inner horizon does not necessarily imply the formation of a singularity. We have proved that a small perturbation has a huge effect on the geometry and leads to the unbounded growth of the Misner–Sharp mass. While in general relativity this usually implies the formation of a singularity, in a full theory of quantum gravity, we might expect the backreaction (perhaps dominated by semiclassical effects [30]) to drive the geometry to a different class of non-singular spacetime [12]. However, in order to address this problem, a geometrical analysis cannot be enough, and we would need to specify the dynamical field equations of a specific theory. Possible quantum gravity frameworks to understand this issue are given by asymptotic safety and loop quantum gravity. In fact, within these theories, there are works predicting regular black holes with an inner horizon [31–36]. These works are mathematically self-consistent as they only deal with vacuum spacetimes, showing that quantum gravity effects can regularize the singularity. However, we have shown in this paper that these analyses are incomplete as the presence of perturbations cannot be ignored. Taking into account the perturbations in a consistent way would be a very demanding but essential computation.

## Acknowledgments

FDF acknowledges financial support by Japan Society for the Promotion of Science Grants-in-Aid for Scientific Research No. 17H06359

SL acknowledges funding from the Italian Ministry of Education and Scientific Research (MIUR) under the grant PRIN MIUR 2017-MB8AEZ.

CP acknowledges: financial support provided under the European Union’s H2020 ERC, Starting Grant agreement no. DarkGRA-757480; support under the MIUR PRIN and FARE programmes (GW-NEXT, CUP: B84I20000100001); support from the Amaldi Research Cen-

ter funded by the MIUR program “Dipartimento di Eccellenza” (CUP: B81I18001170001). MV was supported by the Marsden Fund, via a grant administered by the Royal Society of New Zealand.

---

- [1] R. Penrose, “Gravitational collapse and space-time singularities,” *Phys. Rev. Lett.* **14** (1965) 57–59.
- [2] S. Hawking, “The occurrence of singularities in cosmology. III. Causality and singularities,” *Proc. Roy. Soc. Lond. A* **A300** (1967) 187–201.
- [3] S. W. Hawking and R. Penrose, “The Singularities of gravitational collapse and cosmology,” *Proc. Roy. Soc. Lond. A* **A314** (1970) 529–548.
- [4] **Virgo, LIGO Scientific** Collaboration, B. P. Abbott *et al.*, “Observation of Gravitational Waves from a Binary Black Hole Merger,” *Phys. Rev. Lett.* **116** no. 6, (2016) 061102, [arXiv:1602.03837 \[gr-qc\]](https://arxiv.org/abs/1602.03837).
- [5] **Virgo, LIGO Scientific** Collaboration, B. P. Abbott *et al.*, “GW151226: Observation of Gravitational Waves from a 22-Solar-Mass Binary Black Hole Coalescence,” *Phys. Rev. Lett.* **116** no. 24, (2016) 241103, [arXiv:1606.04855 \[gr-qc\]](https://arxiv.org/abs/1606.04855).
- [6] **VIRGO, LIGO Scientific** Collaboration, B. P. Abbott *et al.*, “GW170104: Observation of a 50-Solar-Mass Binary Black Hole Coalescence at Redshift 0.2” *Phys. Rev. Lett.* **118** no. 22, (2017) 221101, [arXiv:1706.01812 \[gr-qc\]](https://arxiv.org/abs/1706.01812).
- [7] **Virgo, LIGO Scientific** Collaboration, B. P. Abbott *et al.*, “GW170814: A Three-Detector Observation of Gravitational Waves from a Binary Black Hole Coalescence,” *Phys. Rev. Lett.* **119** no. 14, (2017) 141101, [arXiv:1709.09660 \[gr-qc\]](https://arxiv.org/abs/1709.09660).
- [8] **Virgo, LIGO Scientific** Collaboration, B. Abbott *et al.*, “GW170817: Observation of Gravitational Waves from a Binary Neutron Star Inspiral,” *Phys. Rev. Lett.* **119** no. 16, (2017) 161101, [arXiv:1710.05832 \[gr-qc\]](https://arxiv.org/abs/1710.05832).
- [9] R. Carballo-Rubio, F. Di Filippo, S. Liberati, and M. Visser, “Phenomenological aspects of black holes beyond general relativity,” *Phys. Rev. D* **98** no. 12, (2018) 124009, [arXiv:1809.08238 \[gr-qc\]](https://arxiv.org/abs/1809.08238).
- [10] V. Cardoso and P. Pani, “Testing the nature of dark compact objects: a status report,” *Living Rev. Rel.* **22** no. 1, (2019) 4, [arXiv:1904.05363 \[gr-qc\]](https://arxiv.org/abs/1904.05363).
- [11] R. Carballo-Rubio, F. Di Filippo, S. Liberati, and M. Visser, “Opening the Pandora’s box at the core of black holes,” *Class. Quant. Grav.* **37** no. 14, (2020) 145005, [arXiv:1908.03261 \[gr-qc\]](https://arxiv.org/abs/1908.03261).
- [12] R. Carballo-Rubio, F. Di Filippo, S. Liberati, and M. Visser, “Geodesically complete black holes,” *Phys. Rev. D* **101** (2020) 084047, [arXiv:1911.11200 \[gr-qc\]](https://arxiv.org/abs/1911.11200).
- [13] E. Poisson and W. Israel, “Inner-horizon instability and mass inflation in black holes,” *Phys. Rev. Lett.* **63** (1989) 1663–1666.
- [14] A. Ori, “Inner structure of a charged black hole: An exact mass-inflation solution,” *Phys. Rev. Lett.* **67** (1991) 789–792.
- [15] A. J. Hamilton and P. P. Avelino, “The Physics of the relativistic counter-streaming

instability that drives mass inflation inside black holes,” *Phys. Rept.* **495** (2010) 1–32, [arXiv:0811.1926 \[gr-qc\]](https://arxiv.org/abs/0811.1926).

[16] E. G. Brown, R. B. Mann, and L. Modesto, “Mass Inflation in the Loop Black Hole,” *Phys. Rev. D* **84** (2011) 104041, [arXiv:1104.3126 \[gr-qc\]](https://arxiv.org/abs/1104.3126).

[17] R. Carballo-Rubio, F. Di Filippo, S. Liberati, C. Pacilio, and M. Visser, “On the viability of regular black holes,” *JHEP* **07** (2018) 023, [arXiv:1805.02675 \[gr-qc\]](https://arxiv.org/abs/1805.02675).

[18] A. Bonanno, A.-P. Khosravi, and F. Saueressig, “Regular black holes have stable cores,” [arXiv:2010.04226v1 \[gr-qc\]](https://arxiv.org/abs/2010.04226v1).

[19] S. A. Hayward, “Formation and evaporation of regular black holes,” *Phys. Rev. Lett.* **96** (2006) 031103, [arXiv:gr-qc/0506126 \[gr-qc\]](https://arxiv.org/abs/gr-qc/0506126).

[20] C. Barrabès and W. Israel, “Thin shells in general relativity and cosmology: The lightlike limit,” *Phys. Rev. D* **43** (Feb, 1991) 1129–1142. <https://link.aps.org/doi/10.1103/PhysRevD.43.1129>.

[21] R. H. Price, “Nonspherical perturbations of relativistic gravitational collapse. 1. Scalar and gravitational perturbations,” *Phys. Rev. D* **5** (1972) 2419–2438.

[22] R. H. Price, “Nonspherical Perturbations of Relativistic Gravitational Collapse. II. Integer-Spin, Zero-Rest-Mass Fields,” *Phys. Rev. D* **5** (1972) 2439–2454.

[23] A. S. Barreto and M. Zworski, “Distribution of resonances for spherical black holes,” *Mathematical Research Letters* **4** no. 1, (1997) 103–121.

[24] S. Dyatlov, “Asymptotic distribution of quasi-normal modes for kerr–de sitter black holes,” in *Annales Henri Poincaré*, vol. 13, pp. 1101–1166, Springer. 2012.

[25] I. Dymnikova, “Vacuum nonsingular black hole,” *Gen. Rel. Grav.* **24** (1992) 235–242.

[26] V. Cardoso, J. a. L. Costa, K. Destounis, P. Hintz, and A. Jansen, “Quasinormal modes and strong cosmic censorship,” *Phys. Rev. Lett.* **120** (Jan, 2018) 031103. <https://link.aps.org/doi/10.1103/PhysRevLett.120.031103>.

[27] O. J. Dias, F. C. Eperon, H. S. Reall, and J. E. Santos, “Strong cosmic censorship in de Sitter space,” *Phys. Rev. D* **97** no. 10, (2018) 104060, [arXiv:1801.09694 \[gr-qc\]](https://arxiv.org/abs/1801.09694).

[28] S. Hod, “Strong cosmic censorship in charged black-hole spacetimes: As strong as ever,” *Nucl. Phys. B* **941** (2019) 636–645, [arXiv:1801.07261 \[gr-qc\]](https://arxiv.org/abs/1801.07261).

[29] V. Cardoso, J. L. Costa, K. Destounis, P. Hintz, and A. Jansen, “Strong cosmic censorship in charged black-hole spacetimes: still subtle,” *Phys. Rev. D* **98** no. 10, (2018) 104007, [arXiv:1808.03631 \[gr-qc\]](https://arxiv.org/abs/1808.03631).

[30] C. Barceló, V. Boyanov, R. Carballo-Rubio, and L. J. Garay, “Black hole inner horizon evaporation in semiclassical gravity,” [arXiv:2011.07331 \[gr-qc\]](https://arxiv.org/abs/2011.07331).

[31] A. Bonanno and M. Reuter, “Renormalization group improved black hole spacetimes,” *Phys. Rev. D* **62** (Jul, 2000) 043008. <https://link.aps.org/doi/10.1103/PhysRevD.62.043008>.

[32] A. Platania, “Dynamical renormalization of black-hole spacetimes,” *Eur. Phys. J. C* **79** no. 6, (2019) 470, [arXiv:1903.10411 \[gr-qc\]](https://arxiv.org/abs/1903.10411).

[33] A. Held, R. Gold, and A. Eichhorn, “Asymptotic safety casts its shadow,” *JCAP* **06** (2019) 029, [arXiv:1904.07133 \[gr-qc\]](https://arxiv.org/abs/1904.07133).

[34] L. Modesto, “Semiclassical loop quantum black hole,” *Int. J. Theor. Phys.* **49** (2010) 1649–1683, [arXiv:0811.2196 \[gr-qc\]](https://arxiv.org/abs/0811.2196).

- [35] E. Alesci and L. Modesto, “Particle Creation by Loop Black Holes,” *Gen. Rel. Grav.* **46** (2014) 1656, [arXiv:1101.5792 \[gr-qc\]](https://arxiv.org/abs/1101.5792).
- [36] C. Rovelli and F. Vidotto, “Planck stars,” *Int. J. Mod. Phys. D* **23** no. 12, (2014) 1442026, [arXiv:1401.6562 \[gr-qc\]](https://arxiv.org/abs/1401.6562).